RSC Advances

ROYAL SOCIETY OF CHEMISTRY

www.rsc.org/advances

Experimental Design for Simultaneous Analysis of Malachite Green and Methylene Blue; Derivative Spectrophotometry and Principal Component-Artificial Neural Network

M. Ghaedi[a,*], S. Hajati[b,*], M. Zare[a], M. Zare[c], S.Y. Shajaripour Jaberi[a]

[a]*Department of Chemistry, University of Yasouj, Yasouj* 75918-74831*, Iran*

[b]*Department of Physics, University of Yasouj, Yasouj* 75918-74831*, Iran*

[c]*Department of Mechanical Engineering, University of Sistan and Baluchestan, Zahedan, Iran.*

*Corresponding authors. Tel./Fax: +98 74 33223048; E-mail: M. Ghaedi: m_ghaedi@mail.yu.ac.ir and S. Hajati: Hajati@mail.yu.ac.ir

Abstract

In this study, oxidized multiwalled carbon nanotubes (MWCNT) of sizes within the range of 10-30 nm were efficiently applied for simultaneous and competitive adsorption of malachite green (MG) and methylene blue (MB). The competitive adsorption of MB and MG were studied following their accurate and repeatable monitoring in binary mixtures via second order derivative spectrophotometry (SODS) and principal component–artificial neural network model (PCA–ANN). The MWCNTs were characterized by different techniques such as TEM, XPS and FTIR. The dyes removal percentages as responses were modeled and optimized versus the variables by central composite design (CCD) under response surface methodology and PCA–ANN. the optimum values of initial MG and MB concentrations, MWCNT mass (g) and sonication time (min) were found to be 14.6 and 10 mg/L, 0.025 g and 2.6 min, respectively, at which the removal percentages of the dyes were maximum. The advantage of this process is its high removal performance in very short time using small amount of MWCNT. Various isotherm models were applied and their suitability for describing the experimental equilibrium data was investigated. It was shown that the Langmuir model is able to predict real behavior of both dyes in equilibrium mode with removal percentages more than 95% and adsorption capacities of 102.3 and 57.6 mg/g for MB

and MG, respectively.

Keywords: Multiwalled carbon nanotube (MWCNT); Malachite green (MG); Methylene blue (MB); Derivative spectrophotometric; Artificial neural network; Response surface methodology.

1. Introduction

Nanostructuresthere are of high importance and exhaustive applications in versatile fields of science and technology.[1] Nanomaterials are applied in wastewater treatment. Dyes and their photo and/or chemical induced degradation products can seriously affect kidneys, reproductive system, liver, brain, and central nervous system.[2] Cationic toxic dyes of methylene blue (MB, thiazine cationic)[3] and malachite green (MG)[4] (Fig. 1), as reported previously, have numerous medicinal, industrial and biological activities.[4-8] The carcinogenic, genotoxic, mutagenic and teratogenic properties[6-8]of these dyes, which may be related to the presence of nitrogen[5] and positive charge on their structures, were tested on animal as a case study.

Environmental-oriented limiting laws have made it necessary to develop novel and non-toxic materials in a cost-effective and efficient pathway to provide safe and high quality ecosystem.[9] Among various techniques, adsorption process using nanoscale adsorbents could be applied as a promising one to achieve the above-mentioned goals.[10] MWCNTs with high surface area as well as large and wide dimension pores can be a good candidate for wastewater treatment. Therefore, in this work, MWCNTs were used as high performance adsorbent. One of the challenges and requirements in wastewater treatment is the development of novel methods for simultaneous determination and removal of multi-component pollutions from real systems . In such systems, seriously overlapped spectra corresponding to different dyes in their mixtures would cause the lack of accuracy and low repeatability in simultaneous determination of dyes content in the real samples.[11,12]

Therefore, it is necessary to resolve the spectra overlap and overcome these difficulties by using simple spectrophotometric method such as derivative spectrophotometry applied in this study.[13,14,15,16] Central composite design (CCD) was applied under response surface methodology (RSM) to make a predictive model for the simultaneous determination and adsorption of toxic dyes of MG and MB on MWCNTs.

Various isotherm models were applied and their suitability for describing the experimental

equilibrium data was investigated.

2. Experimental

2.1. Instruments and reagents

All chemicals including HCl, NaOH, MG, MB and MWCNTs were purchased from Merck, Darmstadt, Germany. The stock solution of each dye (100 mg/L) was prepared by dissolving 25 mg of the dye in 250 mL double distilled water. It was used as working solution after suitable dilution. The pH/Ion meter (model-827, Metrohm, Swiss), Biochrom UV–Vis spectrophotometer (UK), centrifuge (model T4, Iran), and ultrasonic bath (model Tecna 3, Italy) were used. MWCNT was characterized by transmission electron microscopy (JEM-100CX TEM) and x-ray photoelectron spectroscopy (XPS).

2.2. Central composite design (CCD)

Experimental design is efficiently used for the optimization of responses against variables involved to improve the process performance and minimize error[17,18,19] while running least number of experiments. The significance of parameters including sonication time, amount of MWCNT as adsorbent, MG and MB concentration was investigated by applying the five-level CCD (Table 1) under response surface methodology (RSM) using the Design- Expert software version 7 (Stat-Ease, Minneapolis, USA). In general, the following model may apply to predict any response:[20]

$$Y = \beta_0 + \sum_{i=1}^{3} \beta_i X_i + \sum_{i=1}^{3} \sum_{i \neq j} \beta_{ij} X_i X_j + \sum_{i=1}^{3} \beta_{ii} X_i^2 + \sum_{i=1}^{3} \sum_{j=1}^{3} \sum_{k=1}^{3} \beta_{ijk} X_i X_j X_k \qquad (1)$$

where Y is the predicted response; X_i's are the independent variables. The parameter β_0 is the model constant; β_i's are the linear coefficients; β_{ij} and β_{ijk}'s are the coefficients of interaction terms and β_{ii}'s are the quadratic coefficients.

2.3. Definition of the derivative spectrophotometric (DS)

Seriously overlapped spectra can be resolved by using derivative spectrophotometry.[21,22] Subsequently, calibration curve with high accuracy and repeatability can be obtained. The desired order of derivative is selected and calibration curve for each component is constructed at a wavelength at which the contribution of that component is significant while others are negligible.

2.4. Definition of the PCA–ANN model

PCA and multi-layer ANN perceptron (one hidden layer) are set for the main ANN approach. Also the PCA technique is used to eliminate correlations between rows of the input data and to diminish the input data. In this work, a set of 54 by 341 data was converted to 54 by 4 matrix through PCA to obtain maximum variance in new space according to normalized value [0.1 -1] intervals. MLP-AAN training was achieved by Levenberg-Marquardt with high speed convergence; while the ANN was configured by 0-30 neurons. The mean square error (MSE) is set as a criterion for the ANN performance.

Also, the normalized equation for mapping input data into [0.1- 1] interval is obtained as:

$$X_{normalized} = \frac{X - \min(X)}{\max(X) - \min(X)} \times 0.9 + 0.1 \qquad (2)$$

where matrix X is input data; min(X) and max(X) denote minimum and maximum value of each input data columns, respectively. Then, the ANN outputs are transferred back into origin intervals by renormalizing through the following equation:

$$Output = \frac{ANN_{output} - 0.1}{0.9} \times (\max(\text{targets}) - \min(\text{targets})) + \min(\text{targets}) \qquad (3)$$

After that, weights and biases as the ANN parameters are taken to predict the resultant dyes of experiment with no target. Finally, the removal percentage is available from the results. The ANN procedure is illustrated in Fig. 2.[22]

3. Results and Discussion

3.1. Characterization of adsorbent

MWCNTs (10-20 nm) were oxidized and characterized by TEM, XPS and FTIR. TEM image (Fig. 3) confirms the external and internal diameters of MWCNTs to be 10-20 and 10.5 nm, respectively. IR spectrum of MWCNT shows some important characteristic vibrational frequencies at 3415.31 and 1573.63 corresponding to functional groups of OH and COOH, respectively (Fig. 4) confirmed by C 1s XPS spectrum of the nanotubes (Fig. 5).

3.2. Optimization of pH

The effect of pH on simultaneous adsorption of MB and MG was studied in the pH range of

3.0–8.0. The maximum removal percentages of dyes corresponding to optimum adsorption capacity were obtained at pH 6 (Fig. 6). As known, the occurrence of optimum dyes removal at natural pH which corresponds to working solution of dyes permits to run experiments without any time consuming pH adjustment stage. This fact is promising and could make a great opportunity for the technology of dye removal from natural aqueous dye solutions.

3.3. The simultaneous analysis of MG and MB in binary mixtures by derivative spectrophotometric method

Figure 7 shows the addition of absorbance spectra of single solutions of MG and MB (with a concentration of 7.5 mg/L for each dye) which is not fitted to the absorbance spectrum of their binary solution prepared from 7.5 mg/L of each dye. Therefore, their accurate determination in binary mixture is difficult and has low figures of merit. The derivatives of the spectra (e.g. see Fig. 8a and Fig. 8b for the first and second order derivatives, respectively) were obtained and the wavelength, at which one compound has zero absorbance and the other one contributes in the spectra was found. Thus the absorbance is attributed and proportional to the concentration of other species.[23] The construction of calibration at such wavelength regarding criteria such as determination coefficient and recovery test can judge about suitability of each wavelength. After each differentiation step, a Savitzky-Golay smoothing procedure was applied to obtain a good level of signal-to-noise. Note that, the selected wavelength for MG and MB were 506.1 nm and 602.5 nm, respectively, in the second order derivative spectra (Fig. 8c and Fig. 8d).

The amount of each dye was analyzed via the corresponding calibration curve ($R^2_{MG} = 0.9928$ and $R^2_{MB} = 0.9934$) at the above-mentioned wavelengths. The recoveries (%) and errors (%) between the theoretical (C_t) and measured (C_m) concentrations were calculated using Eqs. **Error! Reference source not found.**) and **Error! Reference source not found.**), respectively.

$$\mathrm{Recovery}(\%) = \frac{c_m}{c_t} \times 100 \qquad (4)$$

$$Error(\%) = \frac{c_m - c_t}{c_t} \times 100 \qquad (5)$$

As seen, reasonably high recovery and low error show the applicability of this method for

accurate analysis and determination of both dyes contents in their binary mixtures (see Table 2).

3.4. Central composite design (CCD)

Four independent variables ((X_1(time), X_2(Adsorbent), X_3(MG concentration), X_4 (MB concentration)) were included in CCD with low, basal and high levels with respective coded values of -1, 0, +1 and the star points of +2 and -2 for +α and -α, respectively. The values of factors and responses are listed in Table 3.

Analysis of variance (ANOVA) was applied for the removal of MG (Table 4) and MB (Table 5). The ANOVA makes it possible to predict the individual, interaction and quadratic effects of all variables on the responses. A p-value less than 0.05 in the ANOVA indicates the statistical significance of a variable at 95% confidence level. After considering the significant terms in Eq. (1), it reduces to the following predictive model for removal percentage (R%) of MG and MB, respectively.

$$R_{MG}\% = 87.74 + 7.99X_2 - 5.9X_4 + 6.45X_2X_3 + 7.85X_2X_4 - 8.58X_3X_4 + 6.41X_2X_3X_4 + 8.97X_1^2X_2 - 8.51X_1^2X_3 \quad (6)$$

$$R_{MB}\% = 86.18 + 5X_2 + 4.39X_2X_3 + 6.03X_2X_4 - 4.89X_3X_4 \quad (7)$$

P-values for lack of fit (LOF) for MG and MB are 0.2007 and 0.0001, respectively. The optimized values of sonication time, adsorbent mass, MG and MB concentration were found to be 2.6 min, 0.025 g, 14.6 and 10 mg/L, respectively. At this condition, the removal percentages for MG and MB were predicted to be 93.85% and 90.03%, respectively, with desirability 1.00. The LOF for the model predicting the removal percentage of MB is significant which may imply the failure of the model. However, to test the validity of the predictions, three experiments were repeated at optimal conditions and the removal percentages for MG and MB were obtained to be 91.75 and 90.12, respectively, indicating good agreement with the predicted. Therefore, both models were validated.

3.5. The simultaneous analysis of MG and MB by PCA-ANN

The simultaneous analysis of MG and MB is performed by PCA-ANN model. It was seen

(Table 6) that the use of 8 neurons leads to best final outcomes. By dividing a MIMO[1]-ANN into some MISO[2]-ANN, the networks are trained to provide desired performance. So the parameters W_{i1}, b_{i1}, W_{i2} *and* b_{i2} ($i = 1, 2$) were set as Tables 6 and 7. Finally, the overall removal percentages of MG and MB are calculated from predicting their concentrations.

As stated before, 54 experiments are considered to train ANN including 70 percent as training data and the remaining as test data. Also, the train and test data are selected randomly. Two activation functions for hidden and output layers are considered as hyperbolic tangent sigmoid and linear, respectively. The number of epochs is set to 1000 iterations. The networks parameters including the coefficients of determination and mean square error (R^2 and MSE) generally give useful knowledge about the applicability of network for repeatable and accurate prediction of real behavior of system:

$$R^2 = 1 - \frac{\sum_{j=1}^{N}\left(y_{prd,j} - y_{\exp,j}\right)}{\sum_{j=1}^{N}\left(y_{prd,j} - y_{m}\right)} \qquad (8)$$

$$MSE = \frac{1}{N}\sum_{i=1}^{N}\left(\left|y_{prd,i} - y_{\exp,i}\right|\right)^2 \qquad (9)$$

where, N is the number of experiment, $y_{prd,i}$ is the output of PCA-ANN and $y_{exp,i}$ is the output of experiment.

The optimal neuron is obtained through try and error by applying various neurons to the ANN and investigating R^2 and MSE. The R^2 and MSE values imply that the use of 8 neurons is the best. According to the designed ANNs (Figs. 9, 10), the R^2 values of 0.9946 and 0.9996 are obtained for MG and MB training, respectively, while the MSE values of 2.29e-04 and 1.6162 are obtained for MG and MB, respectively.

According to R^2 and MSE values, the ANN performance is good enough to use it for predicting the designed experiments by considering four factors, namely initial MG concentration, initial MB concentration, adsorbent dosage (g) and sonication time (min). Table 8 is presented to show the predicted values of two MISO ANNs.

[1] Multi input multi output
[2] Multi input single output

3.6. Application of multi-component adsorption modeling of equilibrium data

Common isotherm models such as Langmuir, Freundlich and Temkin are generally applied to discuss the equilibrium characteristics of the adsorption process.[24] The adsorptions of MG and MB onto MWCNTs in their binary systems were studied at different initial MG and MB concentrations in the range of 8.6 to 16.6 mg/L and 4 to 12 mg/L, respectively, at two different amounts of adsorbent at optimal time (2.6 min). The constant parameters of different isotherms investigated for this adsorption process and the correlation coefficient (R^2) are summarized in Table 9.

Based on the linear form of Langmuir isotherm model (according to Table 9), the values of K_a (the Langmuir adsorption constant (L/mg)) and Q_m (theoretical maximum Monolayer adsorption capacity (mg/g) were obtained from the intercept and slope of the plot of C_e/q_e versus C_e, respectively.

The Freundlich isotherm model can be expressed in linear form (Table 9). The values of K_F (L/mg) and 1/n are determined from the intercept and slope of linear plot of $\log(q_e)$ versus $\log(C_e)$. The high correlation coefficient of Langmuir model at various conditions shows its applicability for the interpretation of experimental equilibrium data.[25] The heat of the adsorption and the adsorbent–adsorbate interaction were evaluated by using Temkin isotherm model.[26] B is the Temkin constant related to heat of the adsorption (J/mol), T is the absolute temperature (K), R is the universal gas constant (8.314 J/mol K), K_T is the equilibrium binding constant (L/mg).

4. Conclusion

In this study, multiwalled carbon nanotubes (MWCNT) were oxidized and used for simultaneous adsorption of malachite green (MG) and methylene blue (MB). The adsorption of MG and MB dyes in their binary mixtures was investigated at batch system at optimized

pH (6.0). The influences of experimental variables on the removal percentages of the dyes were investigated by experimental design methodology. First, the competitive adsorption of MB and MG was studied following evaluation of both dyes content using second order derivative spectrophotometry (SODS). the optimum values of initial MG and MB concentrations, MWCNT mass (g) and sonication time (min) were found to be 14.6 and 10 mg/L, 0.025 g and 2.6 min, respectively, at which the removal percentages of the dyes were maximum.

In the second part, PCA–ANN model as an effective method was applied for the simultaneous prediction of the MG and MB concentrations. The suitability and applicability of the Langmuir model was presented by fitting the experimental equilibrium data to various isotherm models.

The advantage of the process is its high removal performance in very short time using small amount of MWCNT.

5. Acknowledgement

The authors express their appreciation to the Graduate School and Research Council of the University of Yasouj for financial support of this work.

References

1 M. Rahim Nami, M. Janghorban, M. Damadam, , *Aerospace Science and Technology*. 41 (2015) 7-15

2 M. Ghaedi, M. Pakniat, Z. Mahmoudi, S. Hajati, R. Sahraei, A. Daneshfar. *Spectrochimica Acta Part A: Molecular and Biomolecular Spectroscopy*. 123 (2014) 402.

3 M. Roosta, M. Ghaedi, A. Daneshfar, R. Sahraei, A. Asghari. *Ultrasonics Sonochemistry*. 21 (2014) 242.

4 S. Hajati, M. Ghaedi, S. Yaghoubi, Local, J. Ind. Eng. Chem., 21 (2015) 760-767.

5 V. K. Gupta, A. Mittal, L. Krishnan, V. Gajbe, , *Sep. Purif. Technol*. 40 (2004) 87–96.

6 S. J. Culp, L. R. Blankenship, D. F. Kusewitt, D. R. Doerge, L. T. Mulligan, F. A. Beland, *Chem. Biol. Interact*. 122 (1999) 153–170.

7 L. Papinutti, N. Mouso, F. Forchiassin, *Enzyme Microb. Technol*. 39 (2006) 848–853.

8 S. D. Khattri, M. K. Singh, *Adsorp. Sci. Technol*. 17 (1999) 269–282.

9 X. Chen, J.Y. Hu, Water, Air, & Soil Pollution. 206 (2010) 251.

10 Y. Li, K. Sui, R. Liu, X. Zhaoa, Y. Zhang, H. Liang, Y. Xia. *Energy Procedia*.16 (2012) 863.

11 S. Hajati, M. Ghaedi, B. Barazesh, F. Karimi, R. Sahraei, A. Daneshfar, A. Asghari, J. Ind. Eng. Chem. 19 (2013) 227–233.

12 S. Hajati, M. Ghaedi, F. Karimi, B. Barazesh, R. Sahraei, A. Daneshfar, J. Ind. Eng. Chem., 20 (2014) 564-571.

13 S. Hajati, M. Ghaedi, B. Barazesh, F. Karimi, R. Sahraei, A. Daneshfar, A. Asghari, J. Ind. Eng. Chem., 20 (2014) 2421-2427.

14 C.B. Ojeda, F.S. Rojas, *Anal. Chim. Acta*. 518 (2004) 1.

15 S. Sayar, Y. Ozdemir, *Food Chem. J*. 61 (1998) 367.

16 J. Karpinska, *Talanta*. 64 (2004) 801.

17 M. Ghaedi, H. Mazaheri, S. Khodadoust, S. Hajati, M.K. Purkait, Spectrochimica Acta Part A, 135 (2015) 479–490.

18 M. Ghaedi, A. Shahamiri, B. Mirtamizdoust, S. Hajati, F. Taghizadeh, *Spectrochimica Acta A*, 138 (2015) 878-884.

19 A. asfaram, M. Ghaedi, S. Hajati, A. Goudarzi, A.A. Bazrafshan, *Spectrochimica*

Acta A, 145 (2015) 203-212.

20 M. Ghaedi, S. Hajjati, Z. Mahmudi, I. Tyagi, S. Agarwal, A. Maity and V.K. Gupta, *Chem. Eng. J.*, 268 (2015) 28–37.

21 M. Turabik, *J. Hazard. Mater*. 158 (2008) 52.

22 N. Zeinali M. Ghaedi, G. Shafie, *J. Ind. Eng. Chem.* .20 (2014) 3550–3558.

23 M. Turabik. . *J. Hazard. Mater*. 158 (2008) 52-64.

24 M. Ghaedi, S. Zamani Amirabad, F. Marahel, S. Nasiri Kokhdan, R. Sahraei, A. Daneshfar, *Spectrochim. Acta, Part A*. 83 (2011) 46–51.

25 G. McKay, *Chem. Eng. J*. 27 (1983) 187.

26 M. R. Samarghandi, M. Hadi, S. Moayedi, F. Barjasteh Askari, *J. Environ. Health. Sci. Eng*. 6 (2009) 285-294

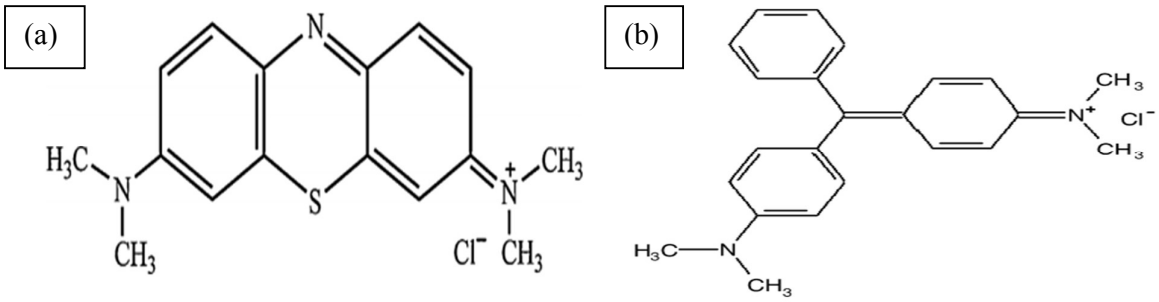

Fig. 1. a) Chemical structure of MB. b) Chemical structure of MG.

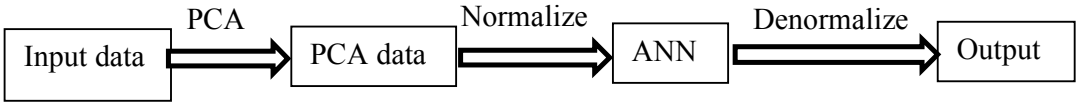

Fig. 2. The PCA-ANN procedure

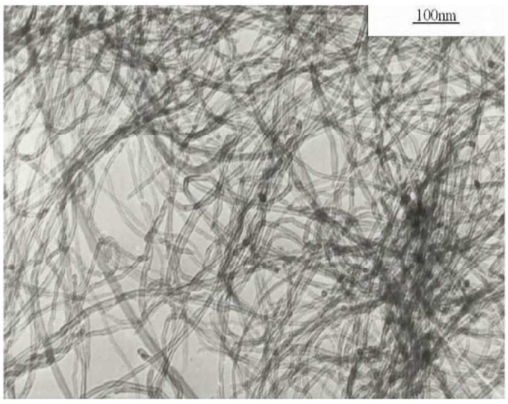

Fig. 3. TEM image of MWCNTs.

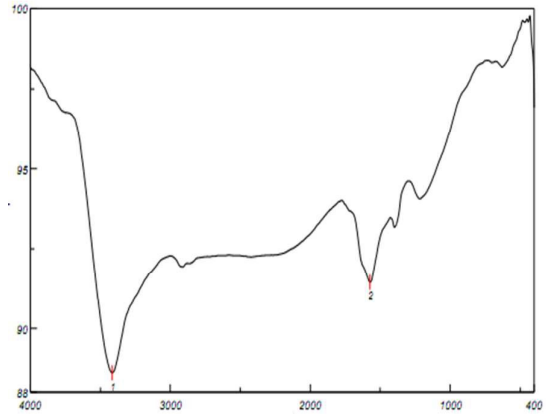

Fig. 4. FTIR spectrum of MWCNTs.

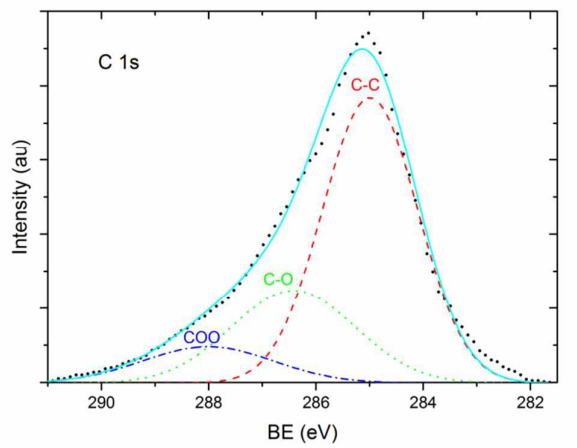

Fig. 5. C 1s XPS spectrum of MWCNTs.

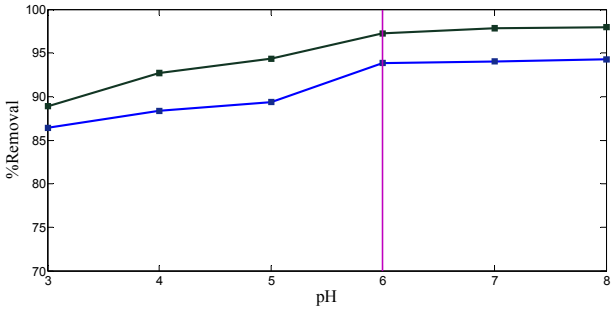

Fig. 6. Effect of pH on the removal of MG and MB MWCNTs, contact time of 4.5 min, adsorbent dosage of 0.02 g in 50 mL and dye concentration of 20 mg/L for each dye**.**

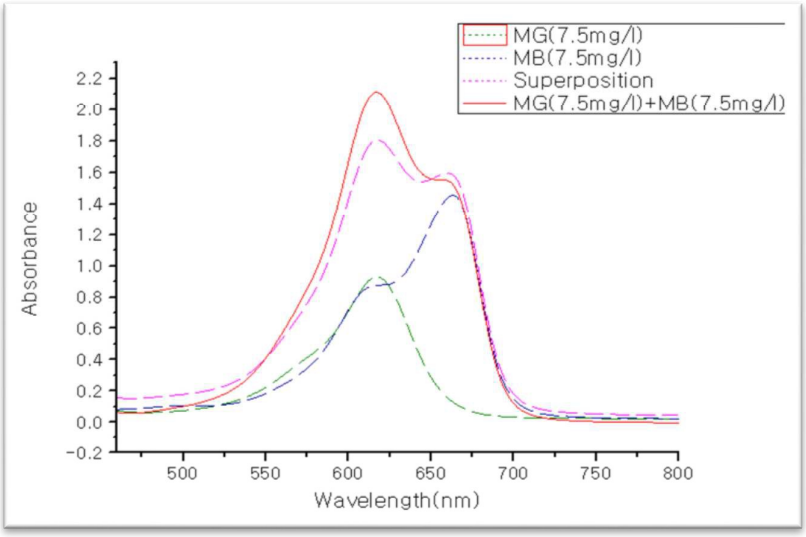

Fig. 7. Zero order absorption spectra of MG and MB in single and binary solutions (initial dye concentration of 7.5 mg/L for each dye).

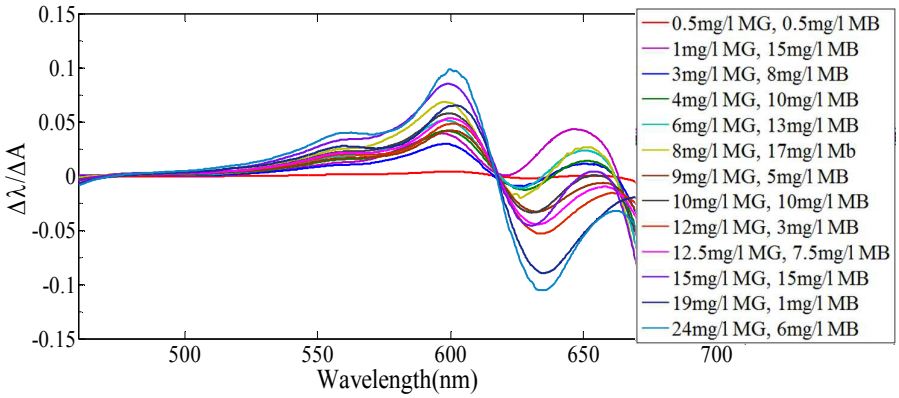

Fig. 8a. First order derivative spectra of MG and MB in binary solution.

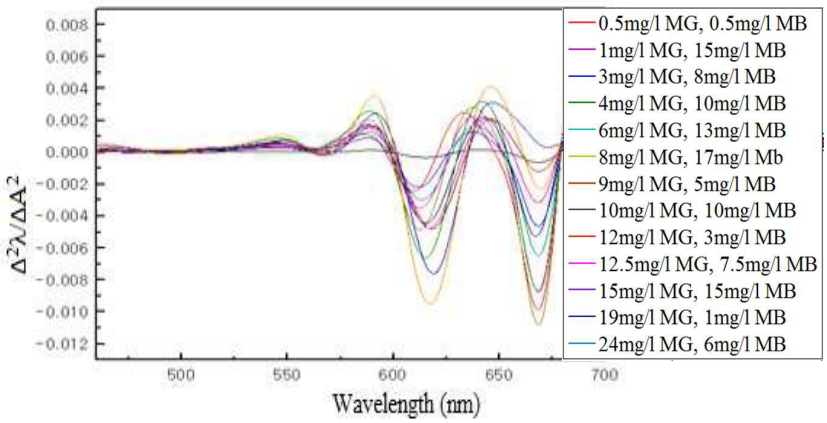

Fig. 8.b. Second order derivative spectra of MG and MB in binary solution.

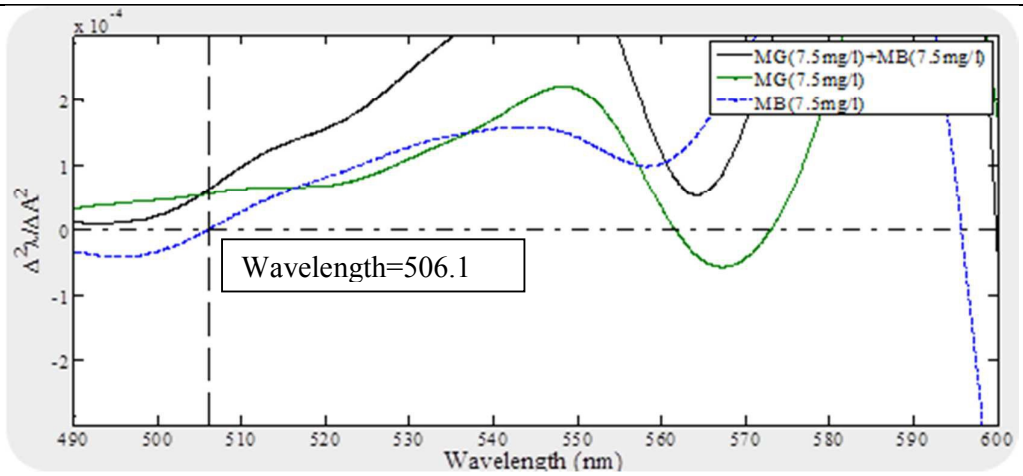

Fig. 8.c. Second order derivative spectra of MG and MB in single and binary solutions (initial dye concentration of 7.5 mg/L)

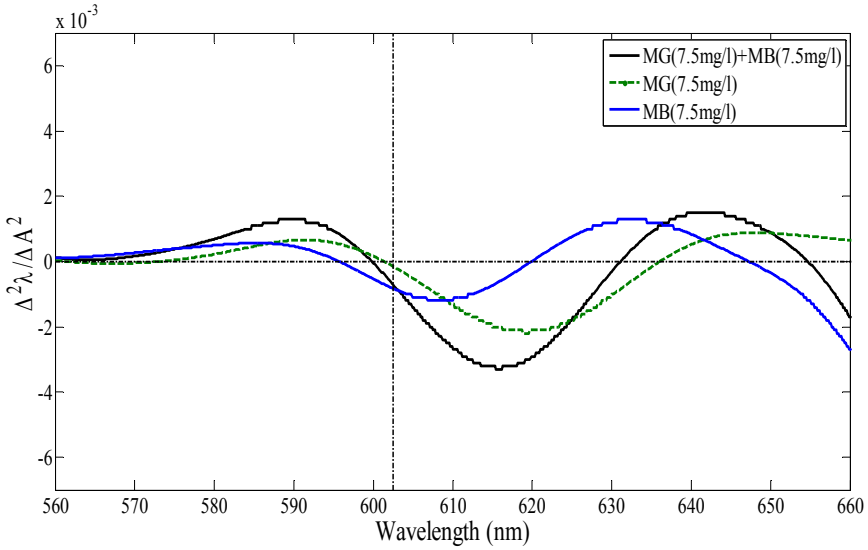

Fig. 8.d. Second order derivative spectra of MG and MB in single and binary solutions (initial dye concentration of 7.5 mg/L)

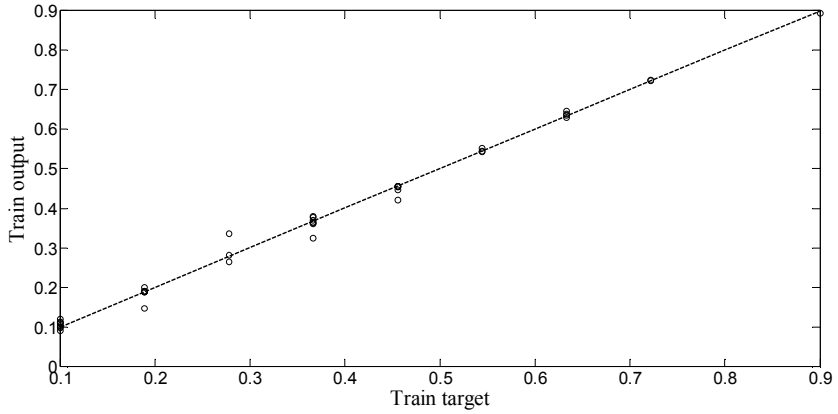

Fig. 9. Performance of the MISO PCA-ANNs for MG

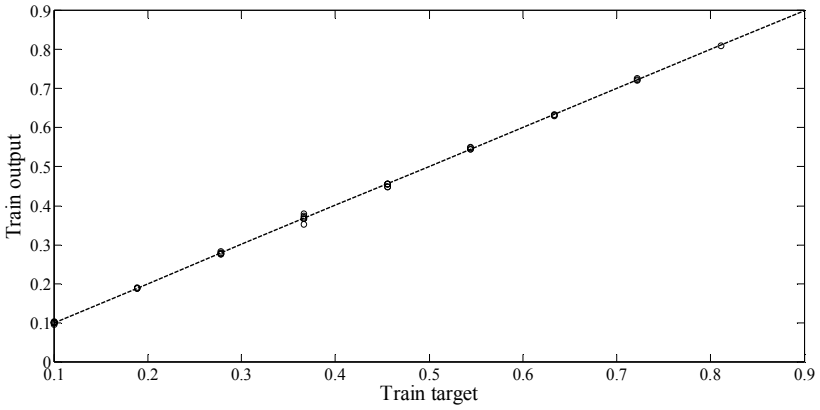

Fig. 10. Performance of the MISO PCA-ANNs for MB

Table 1: Experimental factors and levels in the central composite design.

Factors	level			Star point α=2	
	Low (-1)	central (0)	High (+1)	−α	+α
X_1 (Time)	0.5	2.5	4.5	1.5	3.5
X_2 (Adsorbent)	0.005	0.02	0.035	0.125	0.275
X3 (MG concentration)	5	10	15	7.5	12.5
X4 (MB concentration)	5	10	15	7.5	12.5

Table 2. Recovery and error percentages values for MG and MB in binary mixture obtained by SODS method

Theoretical (mg/L)		Measurement (mg/L)		Recovery (%)		Error (%)	
CMG	CMB	CMG	CMB	MG	MB	MG	MB
7.5	12.5	7.94	12.9	105.86	102.64	5.87	3.2
10	10	8.89	10.01	98.9	102.1	-11.1	0.1
10	10	9.73	8.97	97.3	96.8	-2.7	-10.3
7.5	7.5	6.93	6.73	105.74	89.74	-7.6	-8.27
10	5	9.08	5.09	96.4	97.8	-9.9	1.8
7.5	7.5	7.67	6.99	94.27	103.87	2.27	-6.8
12.5	7.5	12.69	7.78	96	94.4	1.52	3.74
7.5	12.5	7.95	14.48	100.7	104.64	6	15.84
12.5	12.5	12.4	12.07	104.8	88.56	-0.8	-3.44
10	15	10.42	16.9	104.2	106	4.2	12.7
7.5	12.5	6.9	11.99	103.6	102.96	-8	-4.08
10	10	10.05	10.63	91.3	102.3	0.5	6.3
7.5	12.5	8.36	12.31	94.14	96.32	11.47	-1.52
7.5	7.5	7.74	6.52	105.07	89.87	3.2	-13.06
12.5	12.5	13.02	12.85	102.72	98.8	4.16	2.8
5	10	4.83	10.03	102.6	100.3	-3.4	0.3
10	10	9.63	9.01	106.3	103.4	-3.7	-9.9
10	10	10.33	10.02	102.3	90.2	3.3	0.2
12.5	12.5	12.69	12.97	104.24	95.76	1.52	3.76
10	10	9.49	10.18	99.7	101.8	-5.1	1.8
12.5	7.5	12.79	7.37	98.4	105.6	2.32	-1.7
10	10	10.14	10.09	96.4	91	1.4	0.9
10	10	10.65	9.75	98.5	101.5	6.5	-2.5
10	10	9.03	10.98	96.8	97.8	-9.7	9.8
12.5	7.5	12.3	7.69	102.64	94.94	-1.6	2.54
12.5	12.5	13.19	12.06	103.84	98.08	5.52	-3.52
15	10	14.89	1037	106.47	97.9	-0.7	3.7
10	10	9.44	10.32	98.8	93.2	-5.6	2.2
12.5	7.5	13.01	7.31	96	100.14	4.8	2.54
7.5	5	7.69	7.93	105.6	104.7	2.54	5.74

Table 3. Central composite design (CCD)

Run	Time (min)	Adsorbent (g)	Concentration of MG (mg/L)	Concentration of MB (mg/L)	Removal of MG (%)	Removal of MB (%)
1	1.5	0.0275	7.5	12.5	96.20	92.19
2	2.5	0.02	10	10	80.66	91.00
3	2.5	0.005	10	10	65.22	72.06
4	1.5	0.0125	7.5	7.5	79.57	87.26
5	2.5	0.02	10	5	98.45	79.85
6	1.5	0.0275	7.5	7.5	96.91	86.73
7	3.5	0.0275	12.5	7.5	95.62	87.04
8	3.5	0.0275	7.5	12.5	96.38	92.03
9	3.5	0.0125	12.5	12.5	11.52	68.98
10	2.5	0.02	10	15	74.83	90.82
11	1.5	0.0125	7.5	12.5	70.64	86.30
12	2.5	0.02	10	10	81.77	90.69
13	3.5	0.0125	7.5	12.5	74.15	89.65
14	3.5	0.0125	7.5	7.5	79.56	87.41
15	1.5	0.0125	12.5	12.5	10.84	33.33
16	2.5	0.02	5	10	89.74	89.95
17	2.5	0.02	10	10	13.90	90.61
18	2.5	0.02	10	10	.88.59	90.30
19	3.5	0.0275	12.5	12.5	82.90	92.02
20	2.5	0.02	10	10	81.82	90.52
21	3.5	0.0125	12.5	7.5	67.78	89.29
22	0.5	0.02	10	10	59.81	90.03
23	2.5	0.02	10	10	89.08	90.04
24	2.5	0.035	10	10	97.16	89.93
25	1.5	0.0125	12.5	7.5	77.95	89.58
26	1.5	0.0275	12.5	12.5	82.19	92.39
27	2.5	0.02	15	10	87.09	91.12
28	4.5	0.02	10	10	88.48	90.57
29	1.5	0.0275	12.5	7.5	97.56	87.01
30	3.5	0.0275	7.5	7.5	98.52	86.71

Table. 4. Analysis of variance for removal of MG

Source	Sum of squares	df	Mean Square	F Value	p-value Prob > F	
Model	12218.8	12	1018.233	31.47069	< 0.0001	
A-Time	30.76458	1	30.76458	0.950846	0.3432	
B-Adsorbent	510.085	1	510.085	15.76528	0.0010	
C-MG	3.496349	1	3.496349	0.108062	0.7464	
D-MB	278.8854	1	278.8854	8.619553	0.0092	
BC	664.7292	1	664.7292	20.54489	0.0003	
BD	985.5686	1	985.5686	30.46112	< 0.0001	
CD	1176.899	1	1176.899	36.3746	< 0.0001	
B^2	123.1256	1	123.1256	3.805462	0.0678	
BCD	657.7444	1	657.7444	20.32901	0.0003	
A^2B	429.2194	1	429.2194	13.26595	0.0020	
A^2C	386.4311	1	386.4311	11.94349	0.0030	
A^2D	124.0369	1	124.0369	3.833629	0.0669	
Residual	550.0345	17	32.35497			
Lack of Fit	461.7341	12	38.47785	2.178806	0.2007	not significant
Pure Error	88.30032	5	17.66006			
Cor Total	12768.83	29				

Table. 5. Analysis of variance for removal of MB

Source	Sum of Squares	df	Mean Square	F Value	p-value Prob > F	
Model	2163.634	7	309.0905	4.337868	0.0037	
A-Time	64.72473	1	64.72473	0.908366	0.3509	
B-Adsorbent	600.4141	1	600.4141	8.426389	0.0083	
C-MG	183.129	1	183.129	2.570086	0.1232	
D-MB	43.23022	1	43.23022	0.606706	0.4443	
BC	308.2424	1	308.2424	4.325965	0.0494	
BD	581.1627	1	581.1627	8.15621	0.0092	
CD	382.7306	1	382.7306	5.371355	0.0302	
Residual	1567.588	22	71.25402			
Lack of Fit	1567.038	17	92.17868	836.6602	< 0.0001	significant
Pure Error	0.550873	5	0.110175			
Cor Total	3731.222	29				

Table. 6 Tuned weight and bias for hidden and output layer for MB

W_1			W_2	b_1	b_2
-18.29552	12.43589	-3.77786	18.43532	6.23529	0.7253
-16.12921	9.98686	-3.06175	36.10166	5.97259	
-13.69073	7.27125	-2.30438	17.82432	5.68168	
-36.18205	130.52836	68.59978	0.03371	9.91369	
5.15683	-2.37396	-7.73911	-1.25341	4.66208	
1.84681	2.98850	-10.76078	0.98113	5.46931	
-10.67629	7.39008	-7.15177	-0.12935	4.8884	
-58.29830	-16.48420	85.01243	0.06106	24.31207	

Table. 7. Tuned weight and bias for hidden and output layer for MG

W_1			W_2	b_1	b_2
14.04157	-19.07305	-1.67141	32.30820	4.01607	0.11555
-2.99004	23.43434	0.0272	51.48711	-10.9942	
3.85957	4.23926	0.43602	0.93353	-4.66861	
2.80566	23.01649	-0.04299	52.3291	10.875	
14.16208	-19.24329	-1.68804	-31.8603	4.05448	
326.14317	-34.70597	47.21624	0.19873	-166.2270	
-181.6341	171.98565	-179.2723	0.02758	65.75084	
-29.6628	-9.92741	22.29310	-0.12011	-2.12567	

Table. 8. The individual and total adsorption equilibrium uptake and equilibrium concentration for MG and MB in binary mixture obtained by PCA–ANN model.

Run	Time (min)	Adsorbent (g)	Concentration of MG (mg/L)	Concentration of MB (mg/L)	Removal of MG (%)	Removal of MB (%)
1	1.5	0.028	7.5	12.5	93.02	90.44
2	2.5	0.02	10	10	73.69	86.83
3	2.5	0.005	10	10	99.49	92.87
4	1.5	0.013	7.5	7.5	89.82	91.39
5	2.5	0.02	10	5	98.19	85.24
6	1.5	0.028	7.5	7.5	97.59	90.16
7	3.5	0.028	12.5	7.5	95.81	84.07
8	3.5	0.028	7.5	12.5	93.02	90.44
9	3.5	0.013	12.5	12.5	92.42	94.29
10	2.5	0.02	10	15	73.69	95.69
11	1.5	0.013	7.5	12.5	64.93	94.83
12	2.5	0.02	10	10	73.69	93.56
13	3.5	0.013	7.5	12.5	64.93	94.83
14	3.5	0.013	7.5	7.5	89.46	91.39
15	1.5	0.013	12.5	12.5	88.70	94.29
16	2.5	0.02	5	10	89.54	88.05
17	2.5	0.02	10	10	73.69	86.83
18	2.5	0.02	10	10	73.69	86.83
19	3.5	0.028	12.5	12.5	98.99	94.83
20	2.5	0.02	10	10	73.69	93.54
21	3.5	0.013	12.5	7.5	78.95	91.39
22	0.5	0.02	10	10	73.69	93.54
23	2.5	0.02	10	10	73.69	93.56
24	2.5	0.035	10	10	98.74	92.62
25	1.5	0.013	12.5	7.5	78.95	91.39
26	1.5	0.028	12.5	12.5	78.95	94.83
27	2.5	0.02	15	10	94.88	93.54
28	4.5	0.02	10	10	92.36	86.83
29	1.5	0.028	12.5	7.5	93.89	82.44
30	3.5	0.028	7.5	7.5	97.59	90.16

Table. 9 Isotherm parameters for the MG and MB adsorption onto MWCNTs at optimal conditions.

Isotherm	Parameters	Value of parameters			
		0.015		0.025	
		MG	MB	MG	MB
Langmuir	Q_m (mg/g)	16.29	32.79	15.94	16.08
	K_a (L/mg)	1.26	2.52	21.05	7.07
	R^2	0.9713	0.9612	0.9925	0.9858
Freundlich	1/n	0.1536	0.2976	0.1309	0.0155
	K_F (L/mg)	26.37	22.30	17.94	13.29
	R^2	0.7095	0.4894	0.9246	0.0025
Temkin	B_l	3.2861	6.2127	2.5943	0.0375
	K_T (L/mg)	2921.9	43.38	9992.27	370.77
	R^2	0.7646	0.5673	0.9164	1E-04